



Early summer precipitation in the lower Yangtze River basin for AD 1845–2011 based on tree-ring cellulose oxygen isotopes

Chenxi Xu^{1,2} · Jiangfeng Shi^{3,4} · Yesi Zhao³ · Takeshi Nakatsuka⁵ · Masaki Sano^{5,6} · Shiyuan Shi³ · Zhengtang Guo^{1,2,7}

Received: 7 September 2017 / Accepted: 10 April 2018 / Published online: 16 April 2018
© Springer-Verlag GmbH Germany, part of Springer Nature 2018

Abstract

Precipitation from June to August is generally used to reflect the East Asian summer monsoon (EASM) variability. However, the principal modes of the EASM rainfall are different between May–June (MJ) and July–August due to the seasonal march of East Asian subtropical front. Therefore, it is necessary to study them separately. In this study, we reconstruct a 167-year MJ precipitation time series using tree-ring cellulose $\delta^{18}\text{O}$ that explains 46.9% of the variance in the lower Yangtze River basin, Southeast China, that extends the meteorological data back more than 100 years and makes the precipitation study at decadal scales possible. The decades with 5 or more anomalously dry or wet years are the 1880s, 1890s, and 1910s, and the 1980s and 2000s have only one anomalous year per decade. MJ precipitation shows a significantly negative relationship with absolute Niño 3.4 sea surface temperature, especially during the developing phases of El Niño–Southern Oscillation, indicating that there is less rainfall during El Niño events. However, the relationship is not uniform throughout the period. Further analyses show that it is stronger when the Pacific Decadal Oscillation is in its positive phases.

Keywords Tree-ring cellulose oxygen isotope · *Pinus taiwanensis* · May–June precipitation · Lower Yangtze River basin, China · El Niño–Southern Oscillation · Pacific Decadal Oscillation

Electronic supplementary material The online version of this article (<https://doi.org/10.1007/s00382-018-4212-5>) contains supplementary material, which is available to authorized users.

✉ Jiangfeng Shi
shjif@nju.edu.cn

- ¹ Key Laboratory of Cenozoic Geology and Environment, Institute of Geology and Geophysics, Chinese Academy of Sciences, Beijing 100029, China
- ² CAS Center for Excellence in Life and Paleoenvironment, Beijing 100044, China
- ³ School of Geographic and Oceanographic Sciences, Nanjing University, Nanjing 210023, China
- ⁴ Jiangsu Collaborative Innovation Center for Climate Change, Nanjing 210023, China
- ⁵ Research Institute for Humanity and Nature, Motoyama, Kamigamo, Kita-ku, Kyoto, Japan
- ⁶ Faculty of Human Sciences, Waseda University, 2-579-15 Mikajima, Tokorozawa 359-1192, Japan
- ⁷ University of Chinese Academy of Sciences, Beijing 100049, China

1 Introduction

East Asian summer monsoon (EASM) rainfall has a profound influence on the economy of the densely populated regions of East Asia (EA). Tremendous efforts have been made to understand the processes driving the EASM rainfall (Ding and Chan 2005). However, multi-model ensemble predictions of summer precipitation in subtropical–extratropical EA have low skill (Wang et al. 2009). The conventional seasonal forecasts of EASM usually focus on the June–July–August (JJA) anomalies, but a recent study showed that EASM exhibits remarkable differences in its mean states and principal modes of rainfall between early summer (May–June, MJ) and late summer (July–August, JA) due to the seasonal march of EA subtropical front (Wang et al. 2009). Therefore, it is necessary to study early and late summer rainfall variability separately. Wang et al. (2009) identified three principal modes of early summer rainfall anomalies in EA and investigated the links between the principal modes and El Niño–Southern Oscillation (ENSO) based on observations during the period 1979–2007. Li and Zhou (2011) investigated the

predictability of ENSO-related MJ and JA rainfall modes using the output of 12 atmospheric general circulation models during the period 1980–1999. Xing et al. (2017) used an empirical orthogonal function (EOF)-based physical empirical model to investigate the relationship between Pacific sea surface temperature (SST) and MJ rainfall anomalies in EA during the period 1979–2010. The above studies only explore the relationship between ENSO and MJ rainfall anomalies in EA during the last three decades. In order to understand their long-term relationship, it is necessary to extend early summer precipitation records back over hundreds of years.

In EA, historical documents were used for paleo-precipitation reconstruction (Ge et al. 2007), and so were well-dated annually resolved tree ring records (Shi et al. 2015; Xu et al. 2016a). Although the length of the dryness/wetness index (DWI) records from historical documents in eastern China is over several 100 years, DWI is only semi-quantitative (Qian et al. 2006). The summer monthly precipitation in Nanjing, Hangzhou, Suzhou of the eighteenth century has been reconstructed using “Qing Yu Lu” (Zhang and Wang 1989), and the rainfall amount has been reconstructed by the “Yu Xue Fen Cun” records of the Qing dynasty (Ge et al. 2007; Zheng et al. 2016). However, they are limited to a few big cities and are not continuous. Tree ring width is generally temperature-sensitive in eastern China, and has been used to reconstruct temperature changes (Shi et al. 2010, 2013; Duan et al. 2013). Recent research has shown that tree ring width at a low-elevation site in the lower reaches of the Yangtze River has the potential to reconstruct February–April precipitation (Shi et al. 2015). So far, however, reconstruction of MJ precipitation in eastern China has not been attempted.

Tree ring cellulose oxygen isotope ($\delta^{18}\text{O}$) contains information on source water isotope compositions and atmospheric vapor pressure deficit (Roden et al. 2000), which are related to precipitation $\delta^{18}\text{O}$ and relative humidity, respectively (McCarroll and Loader 2004; Liu et al. 2017). Furthermore, precipitation $\delta^{18}\text{O}$ and relative humidity are influenced by monsoon-related precipitation changes in monsoonal Asia (Araguás-Araguás et al. 1998; Liu et al. 2010). Therefore, tree ring $\delta^{18}\text{O}$ holds the potential for monsoon season precipitation reconstruction. The potential has been evidenced by interannual tree ring $\delta^{18}\text{O}$ studies in Thailand, Bhutan, and Southeast China (Sano et al. 2013; Xu et al. 2015, 2016a), and further supported by a recent intra-annual tree ring $\delta^{18}\text{O}$ study (Xu et al. 2016b). Tree ring oxygen isotopes have also been used to analyze interdecadal changes of summer precipitation and investigate the relationship between summer precipitation and ENSO in Japan (Kurita et al. 2016; Sakashita et al. 2016). In this study, we have analyzed tree ring cellulose $\delta^{18}\text{O}$ of *Pinus taiwanensis* in lower Yangtze River basin (LYRB) to investigate

the potential utility of tree ring $\delta^{18}\text{O}$ for MJ precipitation reconstruction, and to identify possible processes driving MJ precipitation over the past 167 years.

2 Materials and methods

2.1 Sampling site and isotope measurements

We collected radial increment cores of *P. taiwanensis* from Baimajian (BMJ, 31.12°N, 116.18°E, 1640–1760 m above sea level (a.s.l.); Fig. 1), which is close to the maximum elevation (1777 m a.s.l.) in the Dabie Mountains. The sampling site is in a narrow distribution band of *P. taiwanensis* trees along mountain ridges above the deciduous forests. Pine trees are generally sparsely distributed. The core samples were dated using conventional techniques in the laboratory (Holmes 1983; Stokes and Smiley 1996). The detailed information on dating and the climatic implications of ring width in the study area can be drawn from Shi et al. (2013).

Four trees (BMJ06, BMJ19, BMJ29, BMJ37) with regular tree-ring width patterns and without missing rings were selected for the isotopic analysis. The modified plate method (Xu et al. 2011, 2013b), based on the chemical treatment procedure of the Jayme–Wise method (Green 1963; Loader et al. 1997), was used to extract α -cellulose. Cellulose samples (sample weight: 80–260 μg) were wrapped in silver foil and tree-ring cellulose oxygen isotope ratios ($^{18}\text{O}/^{16}\text{O}$) were measured using an isotope ratio mass spectrometer (Delta V Advantage, Thermo Scientific) interfaced with a pyrolysis-type high-temperature conversion elemental analyzer (TC/EA, Thermo Scientific) at the Research Institute for Humanity and Nature, Japan. Cellulose $\delta^{18}\text{O}$ values were calculated by comparison with Merck cellulose (laboratory working standard), which was inserted after every eighth tree ring cellulose sample during the measurements. Oxygen isotope results are presented in δ notation as the per mil (‰) deviation from Vienna Standard Mean Ocean Water (VSMOW): $\delta^{18}\text{O} = [(R_{\text{sample}}/R_{\text{standard}}) - 1] \times 1000$, where R_{sample} and R_{standard} are the $^{18}\text{O}/^{16}\text{O}$ ratios of the sample and standard, respectively. The analytical uncertainty for repeated measurements of Merck cellulose (working standard samples) was approximately $\pm 0.14\text{‰}$ ($n = 82$). The mean inter-tree correlation (R_{bar}) and expressed population signal (EPS) were calculated to evaluate the consistency and signal strength of the $\delta^{18}\text{O}$ time series from different trees (Wigley et al. 1984). EPS is a parameter to evaluate the extent of the average of a finite number of time series represent the population average, and generally, a value of 0.85 is one reasonable choice for EPS suggested by Wigley et al. (1984).

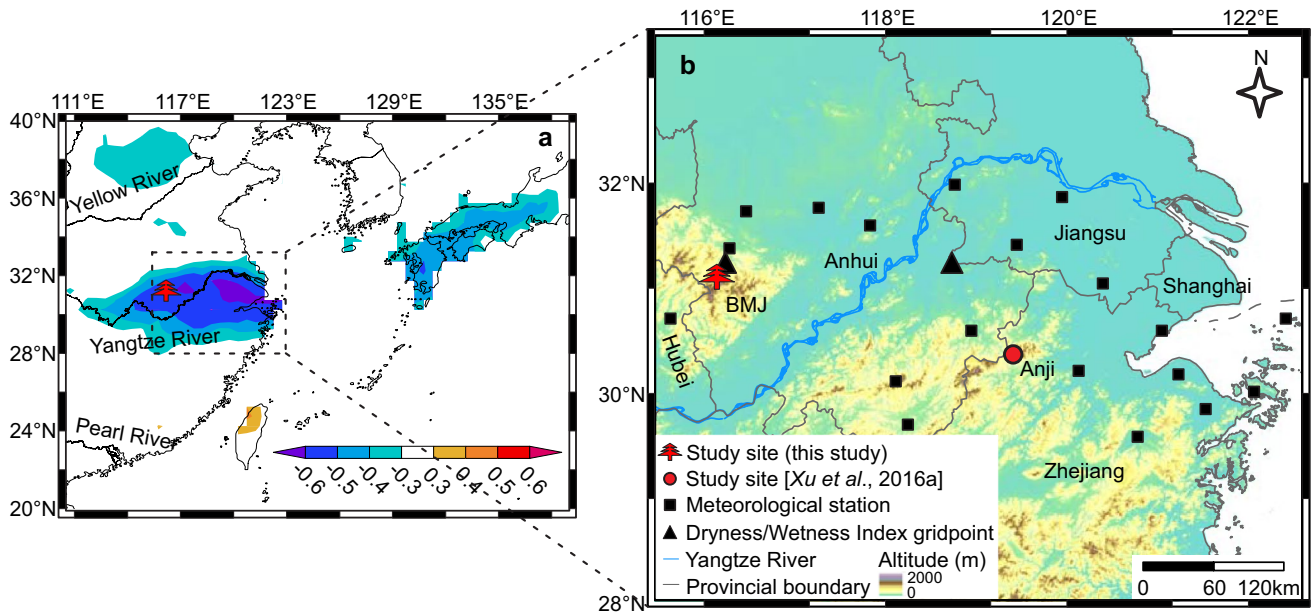


Fig. 1 Overview of the study region. **a** Location of the BMJ sampling site (tree symbol), and the spatial correlations between BMJ tree ring $\delta^{18}\text{O}$ chronology and GPCP v7 precipitation (MJ). **b** Locations of the

19 meteorological stations (square) used for calibration, and the two dryness/wetness index grid points (triangle) used for comparison with our reconstructed MJ precipitation

2.2 Climatic and statistical analyses

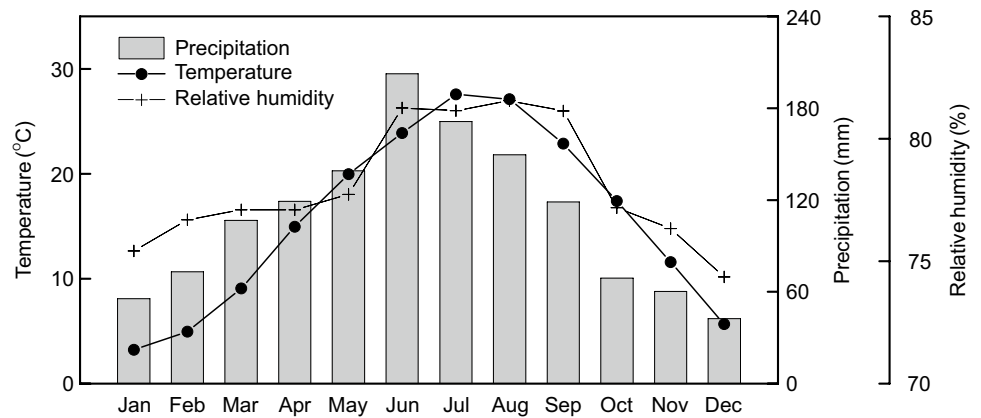
Meteorological data from 19 meteorological stations in LYRB were arithmetically averaged to represent regional climate information (Table 1). The selected weather stations show high degrees of homogeneity in both temperature and precipitation (Li et al. 2004, 2012). Figure 2 illustrates the regional monthly total precipitation, monthly mean temperature, and monthly mean relative humidity from 1951 to 2011. Most precipitation falls from May to August, being highest in June (Fig. 2). To investigate the relationship between tree ring $\delta^{18}\text{O}$ and climatic factors, Pearson’s correlation and response functions were calculated between tree ring $\delta^{18}\text{O}$ series and these three climatic variables, which are thought to be its potential influencing factors (Roden et al. 2000), from January to October over the common period 1951–2011 (Fritts 1976; Biondi and Waikul 2004). Correlation coefficients were also calculated between tree ring $\delta^{18}\text{O}$ series and possible monthly combinations to check out the strongest relationship. The strongest limiting factor, that is MJ precipitation in this study, was chosen as the reconstruction target.

A simple linear regression model was used to transfer tree ring $\delta^{18}\text{O}$ to MJ precipitation. To evaluate the validity of the linear regression model between tree ring $\delta^{18}\text{O}$ and precipitation, two subperiods (1951–1980 and 1981–2011) were used for separate calibration and verification. The Pearson’s correlation coefficient (r), explained variance (R^2), reduction of error (RE), and coefficient of efficiency (CE) were

Table 1 Details of the meteorological stations

Sequence	Name	Latitude	Longitude	Elevation (m a.s.l.)	Time span
1	Yingshan	30.73	115.67	124	1957–2014
2	Chaohu	31.62	117.87	24	1957–2014
3	Hefei	31.78	117.30	27	1953–2014
4	Huangshan	30.13	118.15	1840	1956–2014
5	Huoshan	31.40	116.32	86	1954–2014
6	Lu’an	31.75	116.50	61	1956–2014
7	Ningguo	30.62	118.98	89	1957–2014
8	Tunxi	29.72	118.28	143	1953–2014
9	Pinghu	30.62	121.08	5	1954–2014
10	Cixi	30.20	121.27	5	1954–2014
11	Shengsi	30.73	122.45	80	1959–2014
12	Dinghai	30.03	122.10	36	1955–2014
13	Shengxian	29.60	120.82	104	1953–2014
14	Yinxian	29.87	121.57	5	1953–2014
15	Hangzhou	30.23	120.17	42	1951–2014
16	Nanjing	32.00	118.80	7	1951–2014
17	Changzhou	31.88	119.98	4	1952–2014
18	Liyang	31.43	119.48	8	1953–2014
19	Wuxian-dongshan	31.07	120.43	18	1956–2014

Fig. 2 Monthly total precipitation, monthly mean temperature, and monthly mean relative humidity averaged from the 19 selected meteorological stations for the period 1951–2011



included in statistical tests of calibration and verification (Cook 1985). Precipitation data from GPCP v7 (Schneider et al. 2015) were used to examine the spatial correlation between the oxygen isotope series and MJ precipitation.

To test the validity of our reconstruction, regional MJ precipitation from GPCP v7, the dryness/wetness index (DWI) (Yang et al. 2013), and relevant historical documents were used for comparison. The selected GPCP v7 dataset covers the region 31°–32°N, 115°–122°E, and DWI was averaged from two grid points at 31.25°N, 118.75°E and 31.25°N, 116.25°E. To understand the background circulation conditions associated with MJ precipitation, the SST from the Extended Reconstructed Sea Surface Temperature (ERSST) v4 dataset (Huang et al. 2014), and the 500 hPa geopotential height and 850 hPa wind from the NCEP/NCAR reanalysis dataset (Kalnay et al. 1996), were selected for analysis. In addition, the MJ Niño 3.4 absolute index from the ERSST v4 dataset (Huang et al. 2014) and the reconstructed Pacific

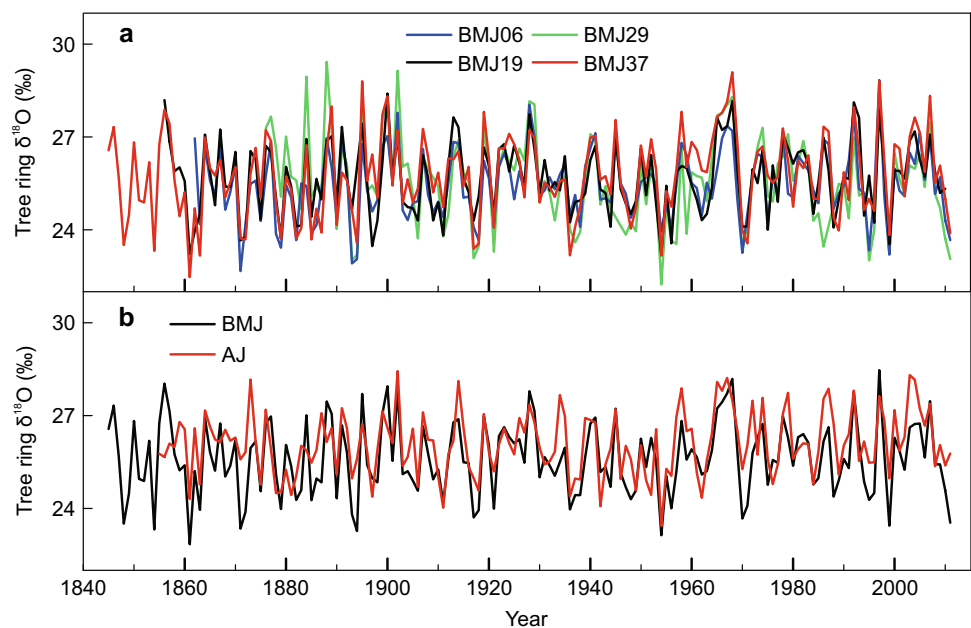
Decadal Oscillation (PDO) index (D'Arrigo and Wilson 2006) were used to explore the possible impact of remote oceans on MJ precipitation.

3 Results and discussion

3.1 Signal strength of tree ring $\delta^{18}\text{O}$

Individual tree-ring cellulose $\delta^{18}\text{O}$ time series from the four cores measured in this study are shown in Fig. 3a. The mean values of the four $\delta^{18}\text{O}$ time series from BMJ06, BMJ19, BMJ29, and BMJ37 are 25.49, 25.69, 25.63, and 25.86‰, respectively, during the common period 1876–2010, while the corresponding standard deviations are 1.10, 1.13, 1.43, and 1.30‰. The yearly $\delta^{18}\text{O}$ standard deviations for the four trees vary between 0.11 and 1.82‰ (mean = 0.55‰). Inter-tree $\delta^{18}\text{O}$ variations show high coherence (Fig. 3a).

Fig. 3 **a** Four individual tree-ring cellulose $\delta^{18}\text{O}$ time series. **b** Comparison of the averaged tree-ring cellulose $\delta^{18}\text{O}$ series in this study (BMJ, black) and the Anji $\delta^{18}\text{O}$ series (AJ, red) (Xu et al. 2016a)



The mean correlation coefficient is 0.77, and the Rbar of the cores are in the range 0.72–0.82 (Table 2). The EPS is 0.93 during the common period 1876–2010, which is higher than 0.85, suggesting that the composite record accurately represents the mean variance of the population (Wigley et al. 1984).

Because the mean value and standard deviation of $\delta^{18}\text{O}$ for the four trees are similar and the $\delta^{18}\text{O}$ time series from the four trees are highly correlated, the four series were then arithmetically averaged to produce the regional $\delta^{18}\text{O}$ chronology (Fig. 3b). The first-order autocorrelation of the $\delta^{18}\text{O}$ chronology is 0.15, which is comparable with the first-order autocorrelation (0.20) of the $\delta^{18}\text{O}$ chronology of *P. taiwanensis* in Anji, Southeast China (Xu et al. 2016a). A low autocorrelation of the $\delta^{18}\text{O}$ chronology indicates that the $\delta^{18}\text{O}$ of the current year is not significantly influenced by processes in the previous year. Our $\delta^{18}\text{O}$ chronology from *P. taiwanensis* trees is positively correlated with the $\delta^{18}\text{O}$ chronology

of *P. taiwanensis* in Anji, Southeast China ($r=0.67$, $n=157$, $p<0.001$; Fig. 3b) (Xu et al. 2016a).

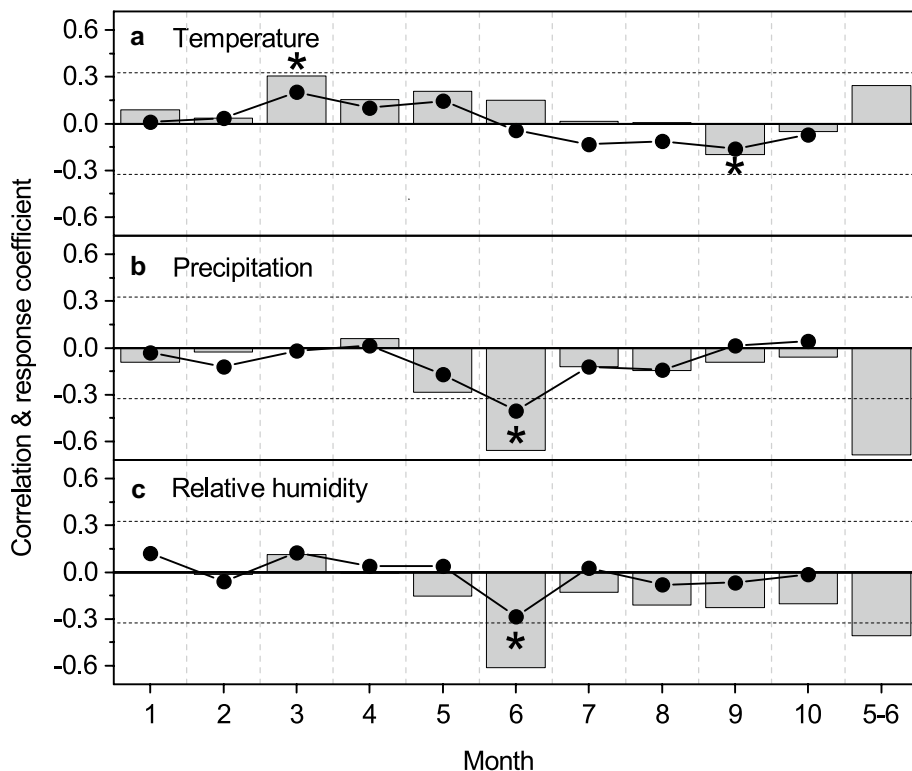
3.2 Climatic response of tree ring $\delta^{18}\text{O}$ and precipitation reconstruction

Correlation and response analyses between the chronology and regional monthly climatic parameters were carried out (Fig. 4). The chronology is significantly negatively correlated with June precipitation and June relative humidity at the 0.01 level, but not significant with any monthly temperature (Fig. 4). May precipitation influences tree ring $\delta^{18}\text{O}$ in the same way as does June precipitation, and so does May relative humidity, even though both at a weaker extent. The correlation coefficient between the chronology and MJ precipitation is -0.69 , higher than that between the chronology and June precipitation, which is -0.66 . Partial correlation analysis was used to evaluate the impact of MJ precipitation on tree ring $\delta^{18}\text{O}$. The coefficient is -0.61 , significant at the 0.01 level when controlling MJ relative humidity. When MJ precipitation was controlled, the partial correlation coefficient between MJ relative humidity and the chronology is -0.06 , not significant even at the 0.05 level. Therefore, MJ precipitation was the strongest influencing factor on tree ring $\delta^{18}\text{O}$. A spatial correlation analysis was further employed to test the regional representativeness of the chronology, showing that it records MJ precipitation in LYRB (Fig. 1a).

Table 2 Correlation coefficients for the four tree ring $\delta^{18}\text{O}$ time series over their common period 1876–2010

	BMJ06	BMJ19	BMJ29
BMJ19	0.78		
BMJ29	0.73	0.72	
BMJ37	0.80	0.82	0.77

Fig. 4 Correlation and response coefficients between the BMJ $\delta^{18}\text{O}$ chronology and **a** monthly mean temperature, **b** monthly total precipitation, and **c** monthly mean relative humidity over 1951–2011. Bar: correlation coefficient; line with dot: response coefficient; horizontal dashed line: the 0.01 significance level for correlation; asterisk: 0.05 significant for response



Negative correlations between tree ring $\delta^{18}\text{O}$ and summer precipitation have also been found in other areas of monsoonal Asia, such as northern Laos (Xu et al. 2013a), northern Vietnam (Sano et al. 2012), northern Thailand (Xu et al. 2015), the Himalayas (Sano et al. 2013), southeast, southwest and northern China (Grießinger et al. 2011; Li et al. 2011; Xu et al. 2013b, 2016a, 2017), and Japan (Yamaguchi et al. 2010; Sakashita et al. 2016).

Precipitation $\delta^{18}\text{O}$ and relative humidity are the main factors affecting tree ring $\delta^{18}\text{O}$ (Roden et al. 2000), and both are related to precipitation amount in summer. Relative humidity usually has a positive relationship with precipitation amount, e.g., the correlation coefficient between regional relative humidity and precipitation in LYRB in MJ was 0.54 ($p < 0.001$) during the period 1951–2011. Increased relative humidity may reduce evapotranspiration, resulting in the source-water and leaf-water being less enriched in isotope composition; consequently, the tree ring $\delta^{18}\text{O}$ becomes lighter (Roden et al. 2000). A negative relationship is usually found between precipitation amount and precipitation $\delta^{18}\text{O}$ in subtropical regions during the rainy season (Dansgaard 1964). This relationship known as the amount effect has also been reported in Nanjing (Tang et al. 2015) and several other sites in Southeast China (Liu et al. 2010). The amount effect is caused by the rainout process, during which condensation processes lead to the preferential removal of heavy water isotopes, thus making the isotope composition of the remaining vapor increasingly lighter (Vuille et al. 2003; Kurita et al. 2009). However, it should be noted that tree ring $\delta^{18}\text{O}$ in BMJ shows a negative correlation with MJ precipitation not only at local sites, but also in the surrounding regions (Fig. 1a). This can be ascribed to the fact that local precipitation $\delta^{18}\text{O}$ is associated with large-scale factors (i.e., upstream atmospheric conditions). Therefore, the use of regionally averaged precipitation would help to identify a clearer relationship with precipitation $\delta^{18}\text{O}$ (Kurita et al. 2009).

MJ precipitation shows the highest correlation with tree ring $\delta^{18}\text{O}$ (Fig. 4), probably because MJ is the peak precipitation period during the growing season. As Zheng et al. (2012) suggested, *P. taiwanensis* in this area grows rapidly in April–July. Of the total rainfall for this stage, 54% falls in MJ and nearly 32% falls in June alone (Fig. 2). Accordingly, MJ precipitation accounts for a larger proportion of rainwater taken up by the trees, and makes the largest variance contribution to tree ring $\delta^{18}\text{O}$.

On the basis of the above analysis, we conclude that MJ precipitation (Pre_{5-6}) is the most appropriate predictand for reconstruction. Thus, a simple linear regression model is used to estimate the transfer function between precipitation and the chronology:

$$\text{Pre}_{5-6} = -60.45\delta^{18}\text{O} + 1895.95;$$

$$(R^2 = 0.469, n = 61, p < 0.001)$$

The model explains 46.9% of observed precipitation variance over the common period 1951–2011. Results of the split calibration–verification test are listed in Table 3. For both sub-periods, statistics such as r and R^2 , are significant ($p < 0.01$), and RE and CE are positive, suggesting the model is valid.

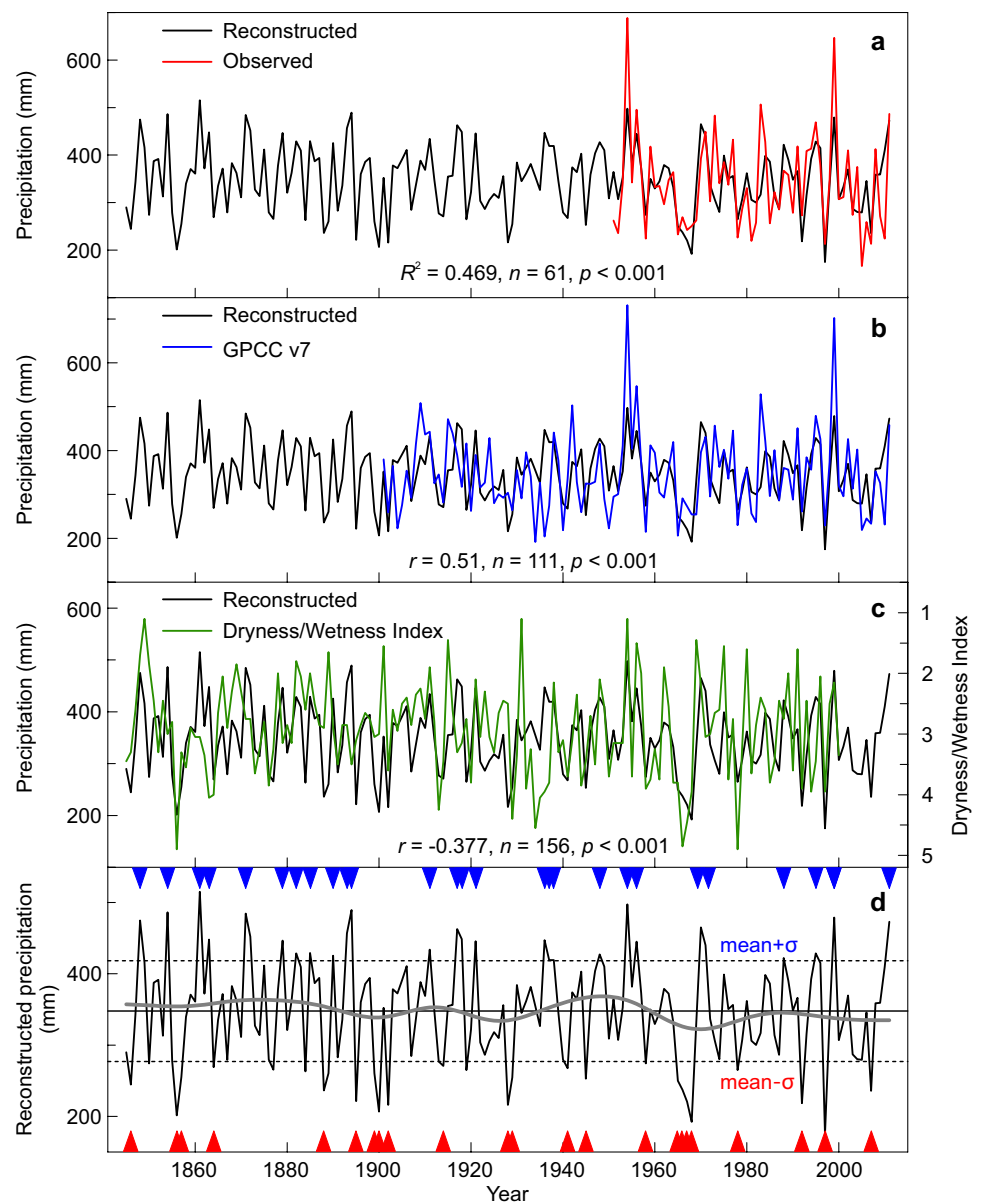
Using the regression model, the annually resolved MJ precipitation was reconstructed for the period 1845–2011 (Fig. 5a). The mean value and standard deviation (σ) of the reconstructed MJ precipitation series are 347.64 and 70.67 mm, respectively. Anomalously wet (dry) years were defined as those with precipitation greater (less) than the mean $+\sigma$ (mean $-\sigma$). With these criteria, 28 anomalously wet years, and the same number of dry years, were identified from the 167-year series (Tables S1 and S2). Anomalous events frequently occurred in the 1880s, 1890s and 1910s (5 events per decade), but seldom in the 1980s and 2000s (only 1 event per decade). The reconstructed series was further smoothed using a 10-year window to highlight the fluctuations at decadal time scales (Fig. 5d). Wet periods with precipitation above the mean value occurred in 1845–1891, 1907–1917, and 1935–1959. Dry periods occurred in 1892–1906, 1918–1934, and 1960–2011.

The correlation coefficients between the reconstructed series and MJ precipitation from GPCC v7 and DWI are 0.51 ($p < 0.001$, 1901–2011) and -0.38 ($p < 0.001$, 1845–2000), respectively (Fig. 5b, c). Extensive historical documentation recorded these defined anomalous precipitation events in Anhui, Jiangsu, Zhejiang, and Hubei provinces, and Shanghai city. Most of the anomalous events had corresponding descriptions in historical documents (Tables S1 and S2; Fig. 5d). All these comparisons suggest that the reconstructed regional MJ precipitation data are reliable and accurate.

Table 3 Calibration and verification statistics for the common period 1951–2011

Calibration period	r	R^2	Verification period	RE	CE
Full period (1951–2011)	-0.685	0.469		–	–
Early half (1951–1980)	-0.737	0.543	Late half (1981–2011)	0.403	0.402
Late half (1981–2011)	-0.638	0.408	Early half (1951–1980)	0.537	0.537

Fig. 5 Comparison of the reconstructed MJ precipitation (black line) with **a** observed MJ precipitation (red line), **b** MJ precipitation from GPCC v7 datasets (blue line), **c** the dryness/wetness index (green line), and **d** documented MJ floods (blue triangle) and droughts (red triangle). The thick grey line in **d** denotes the 10-year smoothed values, and the dashed lines denote the mean ± 1 standard deviations (σ) of the reconstructed precipitation



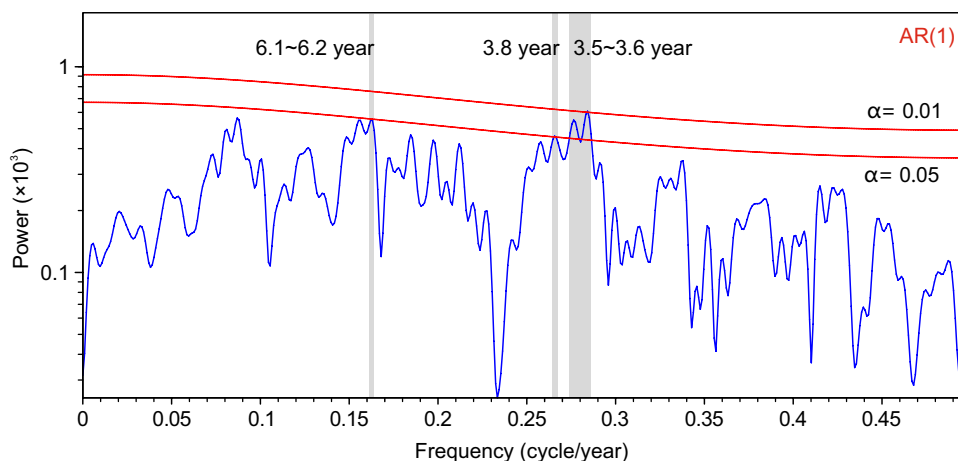
3.3 Relationship with remote oceans

Multi-taper method (MTM) spectral analysis shows that our reconstruction is dominated by significant periodicities at 3.5–3.6 years, 3.8 years, and 6.1–6.2 years (Fig. 6), which fall within the periodicities of ENSO (Li et al. 2013), indicating that MJ precipitation in LYRB may be modulated by ENSO. This is supported by the fact that regional anomalously dry (wet) early summers generally occurred when El Niño (La Niña) events happened in the previous or same year (Tables S1 and S2).

To quantify the influence of ENSO on MJ precipitation during its decaying and developing phases, we calculated the correlation coefficients between MJ precipitation and Niño 3.4 SST in precedent winter (prior December to

February), concurrent MJ, and following winter (December to next February) over the period 1854–2011, which are -0.24 ($p < 0.01$), -0.35 ($p < 0.001$), and -0.33 ($p < 0.001$), respectively. These correlations show that MJ precipitation is more strongly influenced by the developing ENSO than by the decaying ENSO. Composite SST anomalies of anomalously dry and wet years were calculated and are presented in Fig. 7. Positive and negative SST anomalies in the central equatorial Pacific correspond to dry and wet years, respectively. This may be ascribed to the different strength and location of the West Pacific Subtropical High (WPSH) during El Niño and La Niña events. When El Niño (La Niña) events occur, the positive (negative) SST anomalies in the central Pacific and negative (positive) anomalies in the west Pacific weaken (strengthen) the WPSH (Chung et al. 2011;

Fig. 6 Multi-taper method (MTM) spectral analysis of the reconstructed MJ precipitation. Red lines denote the 0.05 and 0.01 significance levels, respectively



Wang et al. 2013; He et al. 2015; Fig. 7g, h). As a result, there is less (more) water vapor supply from the tropical ocean as indicated by the northerly (southerly) wind anomalies (Chang et al. 2000; Fig. 7i, j). Thus, El Niño (La Niña) events cause dry (wet) weather conditions during early summer in LYRB.

However, the negative relationship between reconstructed precipitation and ENSO was not uniform throughout the 158-year period. Based on a 21-year moving correlation analysis, the relationship was strong ($p < 0.05$) in the 1870s, late 1930s–1940s, and 1980s–1990s (Fig. 8a), which correspond to positive PDO phases (Fig. 8b). Analysis based on instrumental records suggest that ENSO's influence on EASM became stronger after the late 1970s when PDO shifted from cool phase to warm phase (Li and He 2001; Xie et al. 2010). These indicate that the stability of ENSO's influence on MJ precipitation may be modulated by PDO at interdecadal timescales. The interdecadal modulation effect of PDO has also been reported when studying the stability of ENSO's influence on early summer precipitation in Japan (Sakashita et al. 2016). The interdecadal change in the relationship between EASM and ENSO during its decaying phase in the late 1970s is attributed to the changes in location and intensity of anomalous convection over the western North Pacific and India (Wu and Wang 2002). However, it remains unclear how PDO modulates the relationship between MJ precipitation in LYRB and ENSO during its developing phase, and the underlying mechanisms should be investigated with coupled atmospheric and oceanic general circulation models.

4 Conclusion

Precipitation is an important issue in LYRB because it can produce floods and can be used to indicate the strength of the EASM which influences lives of billions of people. It is hard to understand its decadal scale variability and driving forces over past several centuries due to the lack of reasonable natural proxies. We have constructed a 167-year *P. taiwanensis* tree-ring cellulose $\delta^{18}\text{O}$ chronology for LYRB, Southeast China. Unlike tree-ring width chronologies which usually reflect temperature variability, the $\delta^{18}\text{O}$ chronology is significantly negatively correlated with regional MJ precipitation over the period 1951–2011. Based on this relationship, a simple linear regression model, with an explained variance of 46.9% of the observed values, has been developed to extend the estimates of MJ precipitation back to 1845. Three decades with 5 or more anomalous precipitation years are recorded in the series. The reconstructed MJ precipitation can be validated by other regional hydroclimatic records around the study region. Even though MJ precipitation is significantly negatively correlated with Niño 3.4 SST over the period 1854–2011, especially in the developing phases of ENSO, the significant relationship is manifested only when PDO is in its warm phases. With the input of longer precipitation reconstructions from more sites in LYRB in the near future, we can have a better understanding of the spatial–temporal characters of the relations at decadal scales.

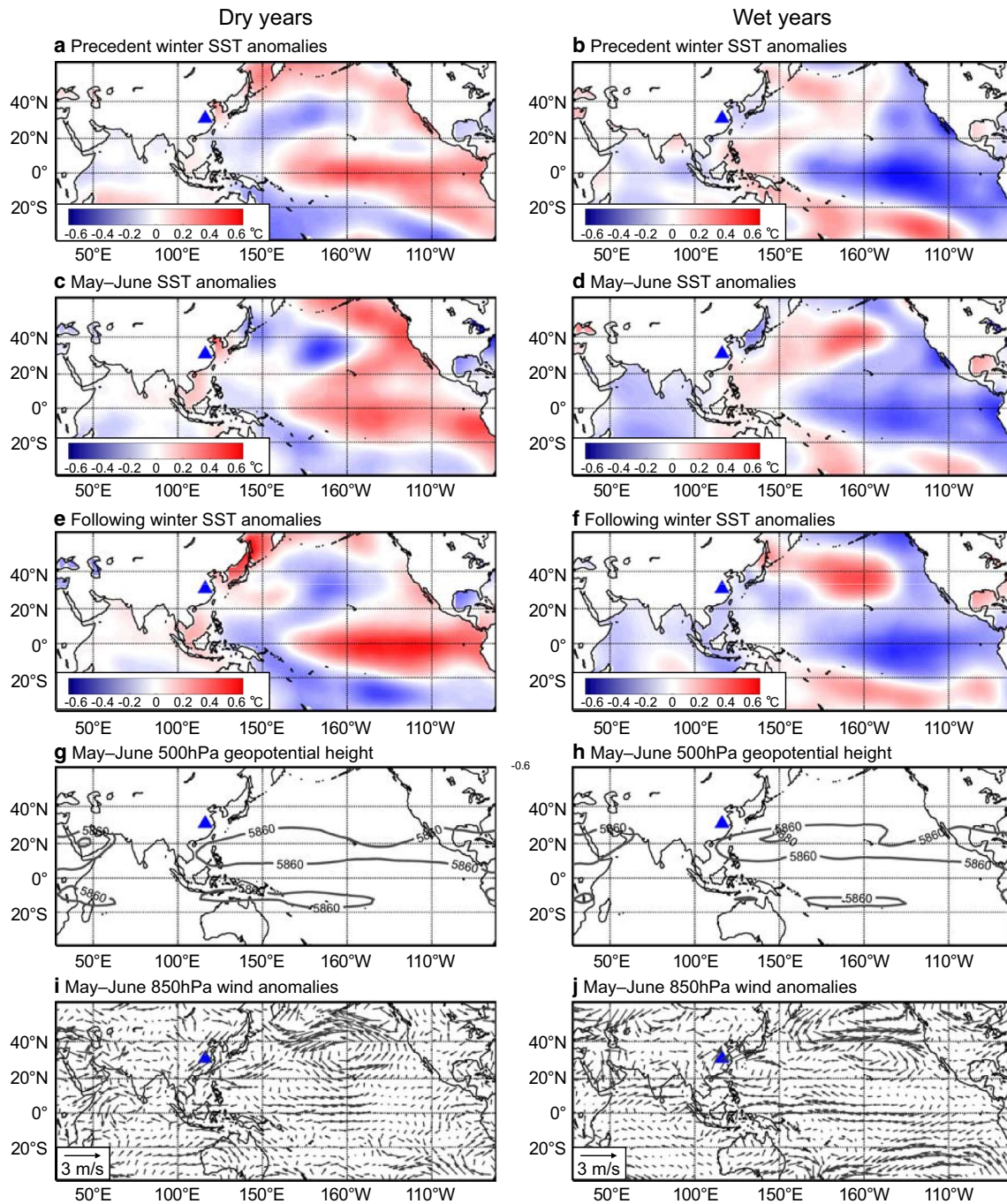
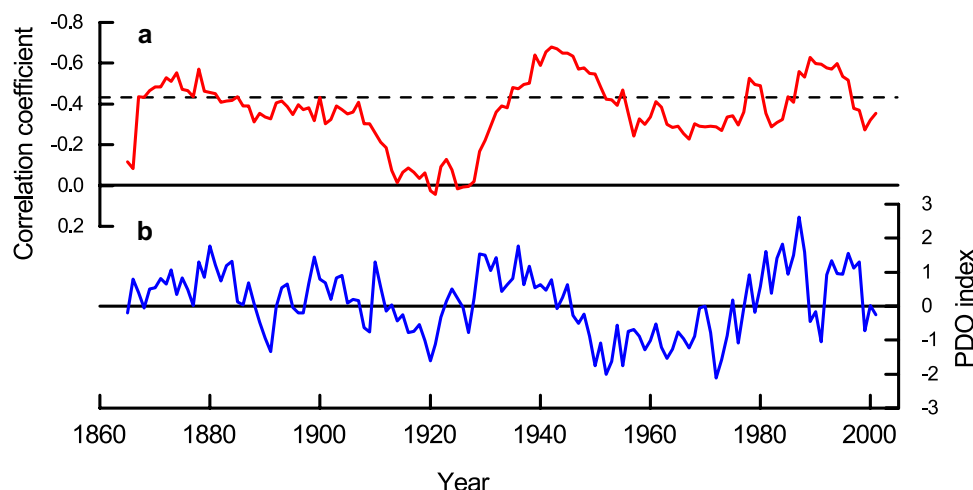


Fig. 7 Composite maps of the precedent winter sea surface temperature (SST) anomalies (a, b), the MJ SST anomalies (c, d), the following winter SST anomalies (e, f), the MJ 500 hPa geopotential height (g, h), and the MJ 850 hPa wind anomalies (i, j). **a, c, e, g** and **i** are

for dry years, and **b, d, f, h** and **j** are for wet years. The SST anomalies were averaged over the period 1854–2011, while 500 hPa geopotential height and 850 hPa wind anomalies were averaged over 1948–2011. The blue triangle represents the BMJ sampling site

Fig. 8 **a** The 21-year moving correlation coefficients between the reconstructed MJ precipitation and the following winter Niño 3.4 SST from ERSST v4 dataset. The dashed line denotes the 0.05 significance level. **b** Reconstructed PDO index (D'Arrigo and Wilson 2006)



Acknowledgements The project was supported by the National Key R&D Program of China (Grant no. 2016YFA0600500), the Chinese Academy of Sciences (CAS) Pioneer Hundred Talents Program, National Natural Science Foundation of China (41671193, 41672179, 41630529, 41430531 and 41690114), and a research grant from the Research Institute of Humanity and Nature, Kyoto, Japan, grant-in-aid for Japan Society for the Promotion of Science Fellows (23242047 and 23-10262). We thank Drs. H. Y. Lu, X. G. Sun, and the anonymous reviewers whose suggestions were helpful in the improvement of the quality of this paper. The tree ring cellulose oxygen isotope data in this paper are available from the authors upon request (shijf@nju.edu.com or cxxu@mail.igccas.ac.cn).

References

- Araguás-Araguás L, Froehlich K, Rozanski K (1998) Stable isotope composition of precipitation over Southeast Asia. *J Geophys Res Atmos* 103(D22):28721–28742. <https://doi.org/10.1029/98JD02582>
- Biondi F, Waikul K (2004) DENDROCLIM2002: A C++ program for statistical calibration of climate signals in tree-ring chronologies. *Comput Geosci* 30(3):303–311. <https://doi.org/10.1016/j.cageo.2003.11.004>
- Chang CP, Zhang YS, Li T (2000) Interannual and interdecadal variations of the East Asian summer monsoon and tropical Pacific SSTs. Part I: roles of the subtropical ridge. *J Clim* 13(24):4310–4325. [https://doi.org/10.1175/1520-0442\(2000\)013<4310:IAI VOT>2.0.CO;2](https://doi.org/10.1175/1520-0442(2000)013<4310:IAI VOT>2.0.CO;2)
- Chung PH, Sui CH, Li T (2011) Interannual relationships between the tropical sea surface temperature and summertime subtropical anticyclone over the western North Pacific. *J Geophys Res Atmos* 116(D13):D13111. <https://doi.org/10.1029/2010JD015554>
- Cook ER (1985) A time series analysis approach to tree ring standardization. Dissertation, University of Arizona
- D'Arrigo R, Wilson R (2006) On the Asian expression of the PDO. *Int J Climatol* 26(12):1607–1617. <https://doi.org/10.1002/joc.1326>
- Dansgaard W (1964) Stable isotopes in precipitation. *Tellus* 16(4):436–468
- Ding Y, Chan JCL (2005) The East Asian summer monsoon: an overview. *Meteorol Atmos Phys* 89(1):117–142. <https://doi.org/10.1007/s00703-005-0125-z>
- Duan J, Zhang QB, Lv LX (2013) Increased variability in cold-season temperature since the 1930s in subtropical China. *J Clim* 26(13):4749–4757. <https://doi.org/10.1175/JCLI-D-12-00332.1>
- Fritts HC (1976) *Tree rings and climate*. Academic, London
- Ge QS, Guo XF, Zheng JY, Hao ZX (2007) Meiyou in the middle and lower reaches of the Yangtze River since 1736. *Chin Sci Bull* 53(1):107–114. <https://doi.org/10.1007/s11434-007-0440-5>
- Green J (1963) *Methods in carbohydrate chemistry*. Academic, New York
- Grießinger J, Bräuning A, Helle G, Thomas A, Schleser G (2011) Late Holocene Asian summer monsoon variability reflected by $\delta^{18}\text{O}$ in tree-rings from Tibetan junipers. *Geophys Res Lett* 38(3):L03701. <https://doi.org/10.1029/2010GL045988>
- He C, Zhou T, Wu B (2015) The key oceanic regions responsible for the interannual variability of the west North Pacific subtropical high and associated mechanisms. *J Meteorol Res* 29(4):562–575. <https://doi.org/10.1007/s13351-015-5037-3>
- Holmes R (1983) Computer-assisted quality control in tree-ring dating and measurement. *Tree-Ring Bull* 43(1):69–78
- Huang B, Banzon VF, Freeman E, Lawrimore J, Liu W, Peterson TC, Smith TM, Thorne PW, Woodruff SD, Zhang H-M (2014) Extended reconstructed sea surface temperature version 4 (ERSST.v4): Part I. Upgrades and intercomparisons. *J Clim* 28(3):911–930. <https://doi.org/10.1175/JCLI-D-14-00006.1>
- Kalnay E, Kanaiitsu M, Kistler R et al (1996) The NCEP/NCAR 40-year reanalysis project. *Bull Am Meteorol Soc* 77:437–470. [https://doi.org/10.1175/1520-0477\(1996\)077<0437:TNYRP>2.0.CO;2](https://doi.org/10.1175/1520-0477(1996)077<0437:TNYRP>2.0.CO;2)
- Kurita N, Ichiyonagi K, Matsumoto J, Yamanaka MD, Ohata T (2009) The relationship between the isotopic content of precipitation and the precipitation amount in tropical regions. *J Geochem Explor* 102(3):113–122. <https://doi.org/10.1016/j.gexplo.2009.03.002>
- Kurita N, Nakatsuka T, Ohnishi K, Mitsutani T, Kumagai T (2016) Analysis of the interdecadal variability of summer precipitation in central Japan using a reconstructed 106 year long oxygen isotope record from tree ring cellulose. *J Geophys Res Atmos* 121(20):12089–12107. <https://doi.org/10.1002/2016JD025463>
- Li F, He J (2001) SST interdecadal change over Pacific area and its relation to East Asian Summer Monsoon. *Sci Meteorol Sin* 21(1):28–35 (in Chinese with English abstract)
- Li B, Zhou T (2011) El Niño–Southern Oscillation-related principal interannual variability modes of early and late summer rainfall over East Asia in sea surface temperature-driven atmospheric general circulation model simulations. *J Geophys Res Atmos* 116(D14):811–840. <https://doi.org/10.1029/2011JD015691>
- Li Q, Liu X, Zhang H, Peterson TC, Easterling DR (2004) Detecting and adjusting temporal inhomogeneity in Chinese mean surface

- air temperature data. *Adv Atmos Sci* 21(2):260–268. <https://doi.org/10.1007/BF02915712>
- Li Q, Nakatsuka T, Kawamura K, Liu Y, Song H (2011) Regional hydroclimate and precipitation $\delta^{18}\text{O}$ revealed in tree-ring cellulose $\delta^{18}\text{O}$ from different tree species in semi-arid Northern China. *Chem Geol* 282(1–2):19–28. <https://doi.org/10.1016/j.chemgeo.2011.01.004>
- Li Q, Peng J, Shen Y (2012) Development of China homogenized monthly precipitation dataset during 1900–2009. *J Geogr Sci* 22(4):579–593. <https://doi.org/10.1007/s11442-012-0948-8>
- Li J, Xie S-P, Cook ER, Morales MS, Christie DA, Johnson NC, Chen F, D'Arrigo R, Fowler AM, Gou X, Fang K (2013) El Niño modulations over the past seven centuries. *Nat Clim Chang* 3:822–826. <https://doi.org/10.1038/nclimate1936>
- Liu JR, Song XF, Yuan GF, Sun XM, Liu X, Wang SQ (2010) Characteristics of $\delta^{18}\text{O}$ in precipitation over Eastern Monsoon China and the water vapor sources. *Chin Sci Bull* 55(2):200–211. <https://doi.org/10.1007/s11434-009-0202-7>
- Liu Y, Cobb KM, Song H et al (2017) Recent enhancement of central Pacific El Niño variability relative to last eight centuries. *Nat Commun* 8:15386. <https://doi.org/10.1038/ncomms15386>
- Loader NJ, Robertson I, Barker AC, Switsur VR, Waterhouse JS (1997) An improved technique for the batch processing of small wholewood samples to α -cellulose. *Chem Geol* 136(3–4):313–317. [https://doi.org/10.1016/S0009-2541\(96\)00133-7](https://doi.org/10.1016/S0009-2541(96)00133-7)
- McCarroll D, Loader NJ (2004) Stable isotopes in tree rings. *Quat Sci Rev* 23(7):771–801. <https://doi.org/10.1016/j.quascirev.2003.06.017>
- Qian W, Yu Z, Zhu Y (2006) Spatial and temporal variability of precipitation in East China from 1880 to 1999. *Clim Res* 32(3):209–218. <https://doi.org/10.3354/cr032209>
- Roden JS, Lin G, Ehleringer JR (2000) A mechanistic model for interpretation of hydrogen and oxygen isotope ratios in tree-ring cellulose. *Geochim Cosmochim Acta* 64(1):21–35. [https://doi.org/10.1016/S0016-7037\(99\)00195-7](https://doi.org/10.1016/S0016-7037(99)00195-7)
- Sakashita W, Yokoyama Y, Miyahara H, Yamaguchi YT, Aze T, Obrochta SP, Nakatsuka T (2016) Relationship between early summer precipitation in Japan and the El Niño–Southern and Pacific Decadal Oscillations over the past 400 years. *Quat Int* 397(4):300–306. <https://doi.org/10.1016/j.quaint.2015.05.054>
- Sano M, Xu C, Nakatsuka T (2012) A 300-year Vietnam hydroclimate and ENSO variability record reconstructed from tree ring $\delta^{18}\text{O}$. *J Geophys Res Atmos* 117(D12):12115. <https://doi.org/10.1029/2012JD017749>
- Sano M, Tshering P, Komori J, Fujita K, Xu C, Nakatsuka T (2013) May–September precipitation in the Bhutan Himalaya since 1743 as reconstructed from tree ring cellulose $\delta^{18}\text{O}$. *J Geophys Res Atmos* 118(15):8399–8410. <https://doi.org/10.1002/jgrd.50664>
- Schneider U, Becker A, Finger P, Meyer-Christoffer A, Rudolf B, Ziese M (2015) GPCC full data reanalysis version 7.0 at 0.5°: monthly land-surface precipitation from rain-gauges built on GTS-based and historic data. https://doi.org/10.5676/DWD_GPCC/FD_M_V7_050
- Shi JF, Cook ER, Lu HY, Li JB, Wright WE, Li SF (2010) Tree-ring based winter temperature reconstruction for the lower reaches of the Yangtze River in southeast China. *Clim Res* 41:169–175. <https://doi.org/10.3354/cr00851>
- Shi J, Cook ER, Li J, Lu H (2013) Unprecedented January–July warming recorded in a 178-year tree-ring width chronology in the Dabie Mountains, southeastern China. *Palaeogeogr Palaeoclimatol Palaeoecol* 381–382(7):92–97. <https://doi.org/10.1016/j.palaeo.2013.04.018>
- Shi J, Lu H, Li J, Shi S, Hou X, Li L (2015) Tree-ring based February–April precipitation reconstruction for the lower reaches of the Yangtze River, Southeast China. *Glob Planet Chang* 131:82–88. <https://doi.org/10.1016/j.gloplacha.2015.05.006>
- Stokes MA, Smiley TL (1996) An introduction to tree-ring dating. University of Arizona Press, Tucson
- Tang Y, Pang H, Zhang W, Li Y, Wu S, Hou S (2015) Effects of changes in moisture source and the upstream rainout on stable isotopes in precipitation—a case study in Nanjing. *Hydrol Earth Syst Sci* 19:4293–4306. <https://doi.org/10.5194/hess-19-4293-2015>
- Vuille M, Bradley RS, Werner M, Healy R, Keimig F (2003) Modeling $\delta^{18}\text{O}$ in precipitation over the tropical Americas: 1. Interannual variability and climatic controls. *J Geophys Res Atmos* 108(D6):4174. <https://doi.org/10.1029/2001JD002038>
- Wang B, Liu J, Yang J, Zhou TJ, Wu ZW (2009) Distinct principal modes of early and late summer rainfall anomalies in East Asia. *J Clim* 22(13):3864–3875. <https://doi.org/10.1175/2009JCL12850.1>
- Wang B, Xiang B, Lee JY (2013) Subtropical high predictability establishes a promising way for monsoon and tropical storm predictions. *Proc Natl Acad Sci USA* 110(8):2718–2722. <https://doi.org/10.1073/pnas.1214626110>
- Wigley TML, Briffa KR, Jones PD (1984) On the average value of correlated time series, with applications in dendroclimatology and hydrometeorology. *J Clim Appl Meteorol* 23(2):201–213
- Wu R, Wang B (2002) A Contrast of the East Asian Summer Monsoon-ENSO relationship between 1962–77 and 1978–93*. *J Clim* 15(15):3266–3279. [https://doi.org/10.1175/1520-0442\(2002\)015<3266:ACOTEA>2.0.CO;2](https://doi.org/10.1175/1520-0442(2002)015<3266:ACOTEA>2.0.CO;2)
- Xie S-P, Du Y, Huang G, Zheng X-T, Tokinaga H, Hu K, Liu Q (2010) Decadal shift in El Niño influences on Indo-Western Pacific and East Asian climate in the 1970s*. *J Clim* 23(12):3352–3368. <https://doi.org/10.1175/2010jcli3429.1>
- Xing W, Wang B, Yim SY, Ha KJ (2017) Predictable patterns of the May–June rainfall anomaly over East Asia. *J Geophys Res Atmos* 122(4):2203–2217. <https://doi.org/10.1002/2016JD025856>
- Xu C, Sano M, Nakatsuka T (2011) Tree ring cellulose $\delta^{18}\text{O}$ of *Fokienia hodginsii* in northern Laos: a promising proxy to reconstruct ENSO? *J Geophys Res Atmos* 116(D24):D24109. <https://doi.org/10.1029/2011JD016694>
- Xu C, Sano M, Nakatsuka T (2013a) A 400-year record of hydroclimate variability and local ENSO history in northern Southeast Asia inferred from tree-ring $\delta^{18}\text{O}$. *Palaeogeogr Palaeoclimatol Palaeoecol* 386:588–598. <https://doi.org/10.1016/j.palaeo.2013.06.025>
- Xu C, Zheng H, Nakatsuka T, Sano M (2013b) Oxygen isotope signatures preserved in tree ring cellulose as a proxy for April–September precipitation in Fujian, the subtropical region of southeast China. *J Geophys Res Atmos* 118(23):12805–12815. <https://doi.org/10.1002/2013JD019803>
- Xu C, Pumijumnong N, Nakatsuka T, Sano M, Li Z (2015) A tree-ring cellulose $\delta^{18}\text{O}$ -based July–October precipitation reconstruction since AD 1828, northwest Thailand. *J Hydrol* 529:433–441. <https://doi.org/10.1016/j.jhydrol.2015.02.037>
- Xu C, Ge J, Nakatsuka T, Yi L, Zheng H, Sano M (2016a) Potential utility of tree ring $\delta^{18}\text{O}$ series for reconstructing precipitation records from the lower reaches of the Yangtze River, southeast China. *J Geophys Res Atmos* 121(8):3954–3968. <https://doi.org/10.1002/2015JD023610>
- Xu C, Zheng H, Nakatsuka T, Sano M, Li Z, Ge J (2016b) Inter- and intra-annual tree-ring cellulose oxygen isotope variability in response to precipitation in Southeast China. *Trees* 30(3):785–794. <https://doi.org/10.1007/s00468-015-1320-2>
- Xu C, Zhu H, Nakatsuka T, Sano M, Zhen L, Shi F, Liang E, Guo Z (2017) Sampling strategy and climatic implication of tree-ring cellulose oxygen isotopes of *Hippophae tibetana* and *Abies georgei* on the southeastern Tibetan Plateau. *Int J Biometeorol*. <https://doi.org/10.1007/s00484-017-1365-6>
- Yamaguchi YT, Yokoyama Y, Miyahara H, Sho K, Nakatsuka T (2010) Synchronized Northern Hemisphere climate change and solar magnetic cycles during the Maunder minimum. *Proc Natl*

- Acad Sci USA 107(48):20697–20702. <https://doi.org/10.1073/pnas.1000113107>
- Yang F, Shi F, Kang S, Wang S, Xiao Z, Nakatsuka T, Shi J (2013) Comparison of the dryness/wetness index in China with the Monsoon Asia Drought Atlas. *Theor Appl Climatol* 114(3–4):553–566. <https://doi.org/10.1007/s00704-013-0858-4>
- Zhang D, Wang PK (1989) Reconstruction of the eighteenth century summer monthly precipitation series of Nanjing, Suzhou, and Hangzhou using the clear and rain records of Qing Dynasty. *J Meteorol Res* 3(3):261–278
- Zheng Y, Zhang Y, Shao X, Yin Z-Y, Zhang J (2012) Temperature variability inferred from tree-ring widths in the Dabie Mountains of subtropical central China. *Trees* 26(6):1887–1894. <https://doi.org/10.1007/s00468-012-0757-9>
- Zheng J-Y, Sun D, Liu K-B, Hao Z-X, Zhang X-Z, Ge Q-S (2016) Variations of extreme Meiyu events and floods disasters over the Mid-lower Reaches of the Yangtze River for the past 300 years. *J Nat Resour* 31(12):1971–1983. <https://doi.org/10.11849/zrzyxb.20161122> (in Chinese with English abstract)